ORIGINAL ARTICLE

Cancer Science WILEY

Endoscopic near-infrared photoimmunotherapy in an orthotopic head and neck cancer model

Ryuhei Okada 🆔 | Aki Furusawa | Fuyuki Inagaki 🆔 | Hiroaki Wakiyama 🆔 | Takuya Kato | Shuhei Okuyama | Hideyuki Furumoto | Hiroshi Fukushima | Peter L. Choyke | Hisataka Kobayashi 🆔

Molecular Imaging Branch, Center for Cancer Research, National Cancer Institute, National Institutes of Health, Bethesda, MD, USA

Correspondence
Hisataka Kobayashi, National Institutes of Health, Building 10, Room B3B69, MSC 1088, 10 Center Drive, Bethesda, MD 20892, USA.
Email: kobayash@mail.nih.gov

Abstract

Near-infrared photoimmunotherapy (NIR-PIT) is a cell selective cancer therapy that uses an antibody-photoabsorber (IRDye700DX, IR700) conjugate (APC) and NIR light. NIR-PIT targeting epidermal growth factor receptor (EGFR) in head and neck cancer (HNC) was conditionally approved in Japan in 2020. APC-bound tumors can be detected using endoscopic fluorescence imaging, whereas NIR light can be delivered using endoscopic fiber optics. The aims of this study were: (1) to assess the feasibility of endoscopic NIR-PIT in an orthotopic HNC model using a CD44-expressing MOC2-luc cell line; and (2) to evaluate quantitative fluorescence endoscopic imaging prior to and during NIR-PIT. The results were compared in 3 experimental groups: (1) untreated controls, (2) APC injection without light exposure (APC-IV), and (3) APC injection followed by NIR light exposure (NIR-PIT). APC injected groups showed significantly higher fluorescence signals for IR700 compared with the control group prior to therapeutic NIR light exposure, and the fluorescence signal significantly decreased in the NIR-PIT group after light exposure. After treatment, the NIR-PIT group showed significantly attenuated bioluminescence compared with the control and the APC-IV groups. Histology demonstrated diffuse necrotic death of the cancer cells in the NIR-PIT group alone. In conclusion, endoscopically delivered light combined with quantitative fluorescence imaging can be used to "see and treat" HNC. This method could also be applied to other types of cancer approachable with endoscopy.

KEYWORDS
endoscopy, murine oral cancer, oral cancer, photoimmunotherapy

1 | INTRODUCTION

HNC is the seventh most common cancer worldwide with >932 000 new cases in 2020; more than 60% of patients are initially diagnosed with advanced stage disease.[1,2] Traditionally, surgery, chemotherapy, and radiotherapy are the cornerstones of treatment for HNC. In the past few decades, however, several additional options have been added to the treatment regimen. A monoclonal antibody against EGFR, cetuximab, was approved in 2006 by the US Food and Drug Administration (US FDA).[3] The first immune checkpoint inhibitor for HNC, nivolumab, was approved by the FDA in 2016.[4] Progress in surgery has also occurred with the introduction of robotic and endoscopy-assisted surgery to enable less invasive local resection.[5,6] In spite of these advances, a considerable number of patients continue to succumb to HNC with high morbidity and mortality; more than 467 000 patients died from HNC worldwide in 2020.[2] Therefore, a new treatment strategy is needed.

Near-infrared photoimmunotherapy (NIR-PIT) is a biotechnology that enables selective and local destruction of targeted cells using an antibody-photoabsorber (IRDye700DX, IR700) conjugate (APC) and NIR light.[7] After intravenous administration, the APC binds to the surface of target cells and subsequent NIR light exposure induces necrotic and immunogenic cell death.[8,9] A global phase III clinical trial of NIR-PIT targeting EGFR in inoperable or recurrent HNC is currently underway (https://clinicaltrials.gov/ct2/show/NCT03769506). The first APC for human use, cetuximab-IR700 (ASP-1929, Akalux™, Rakuten Medical Inc), in combination with a near-infrared laser system (BioBlade™, Rakuten Medical Inc) were conditionally approved for clinical use by the Pharmaceuticals and Medical Devices Agency (PMDA) in Japan in 2020. Although this treatment is currently approved only for inoperable or recurrent HNC, it is a promising therapy for early stage HNCs as well.

CD44 is a well known cancer stem-like cell marker and its high expression on cancer cells correlates with poor prognosis, particularly in HNC.[10-12] In preclinical studies, CD44-targeted NIR-PIT showed in vivo therapeutic efficacy against subcutaneously established syngeneic murine oral cancer models, such as MOC1 or MOC2-luc.[13,14] However, its efficacy against an orthotopic model, which reflects a more realistic tumor microenvironment,[15] has not been proven to date.

During NIR-PIT, NIR light is applied to the tumor that for superficial lesions can be accomplished with a frontal light diffuser. For deeper lesions a cylindrical light diffuser catheter can be placed interstitially within the tumor. For lesions that can be approached endoscopically (eg, HNC or esophageal cancer) light from a cylindrical diffuser can be delivered to the lesion through the endoscope, with which magnified views can be obtained to detect small lesions. For lesions deep in the mouth or near the vocal cords, an endoscopic approach of localizing and treating the cancer is practical. However, the feasibility of endoscopic NIR-PIT against HNC has not been assessed in the preclinical setting. Also,

fluorescence imaging prior to light exposure is a useful strategy to detect the true extent of the lesion, because IR700 is also a fluorescent dye that can be imaged.[16] The utility of a fluorescence endoscopy system optimized to IR700 has been previously reported.[17] In the current study, we combined this endoscopic system and newly developed software to quantitatively assess the fluorescence of IR700 in real time. As IR700 fluorescence is photobleached during successful NIR-PIT, fluorescence imaging is a method of monitoring the completeness of NIR-PIT,[18] Therefore, real-time measurement of the fluorescence signal of IR700 could provide important information to the user on the appropriate light dose for each tumor.

The aim of this study was first to assess the therapeutic efficacy and feasibility of endoscopic NIR-PIT in an orthotopic HNC model using a CD44-expressing MOC2-luc tumor and second to evaluate the usefulness of endoscopic quantitative real-time fluorescence signals in guiding NIR-PIT.

2 | MATERIALS AND METHODS

2.1 | Reagents

The IR700 NHS ester was obtained from LI-COR Biosciences (Lincoln, NE, USA). Anti-mouse-CD44 antibody (IM7) was purchased from Bio X Cell (West Lebanon, NH, USA). All other chemicals were of reagent grade.

2.2 | Synthesis of APC

Anti-CD44 antibody (1 mg, 6.8 nmol) was incubated with a 5-fold molar excess of IR700 NHS ester in phosphate buffer (pH 8.5) at room temperature for 1 h. The mixture was purified on a Sephadex G25 column (PD-10; GE Healthcare, Piscataway, NJ, USA). Anti-CD44 antibody conjugated with IR700 is referred to as anti-CD44-IR700.

2.3 | Cell culture

The MOC2 cell line (murine oral cancer) was purchased from Kerafast (Boston, MA, USA) and luciferase was transduced with RediFect Red-Fluc lentivirus (PerkinElmer, Waltham, MA, USA). The resulting cell line is referred to as MOC2-luc. The cells were cultured in a mixture of Iscove's Modified Dulbecco's Medium (IMDM) and Ham's Nutrient Mixture F12 Medium (at a ratio of 2:1, GE Health Healthcare Life Sciences) supplemented with 5% fetal bovine serum (Thermo Fisher Scientific, Rockford, IL, USA), 1% penicillin/streptomycin (Thermo Fisher Scientific), 5 ng/mL insulin (Millipore Sigma, Burlington, MA, USA), 40 ng/mL hydrocortisone (Millipore Sigma), and 3.5 ng/mL human recombinant epidermal growth factor (EGF) (Millipore Sigma). Cells were cultured in a humidified incubator at 37°C in an atmosphere of 95% air and 5% CO_2.

2.4 | Cell-specific binding analysis

One million MOC2-luc cells were incubated with 10 μg/mL anti-CD44-IR700 for 30 min at 4°C. After washing with PBS, the fluorescence of the cells was analyzed using a flow cytometer (FACSLyric, BD Biosciences, San Jose, CA, USA) and FlowJo software (BD Biosciences). To confirm the specific binding of the anti-CD44-IR700, a 10-fold excess of unconjugated anti-CD44 antibody was added to some samples 30 min prior to the administration of the APC.

2.5 | In vitro NIR-PIT

MOC2-luc cells (2×10^4) were seeded into glass-bottomed 6-well plates and incubated for 1 d. Then, the cells were incubated with 10 μg/mL anti-CD44-IR700 for 1 h at 37°C. The cells were washed with PBS and observed under a microscope (BX61; Olympus America, Melville, NY, USA). The cells were then exposed to NIR light (690 nm, 100 mW/cm, 1 J/cm) using an RD30 cylindrical diffuser (Medlight, Ecublens, Switzerland) and an ML7710 laser system (Modulight, Tampere, Finland). Morphological changes were observed with transmitted light differential interference contrast (DIC) images. IR700 fluorescence was detected using a combination of a 590-650 nm excitation filter and a 665-740 nm band pass emission filter. For quantitative analysis of cytotoxicity, MOC2-luc cells (2×10^5) were aliquoted in 500 μL of 1% FBS in PBS. Then, the cells were incubated with 10 μg/mL anti-CD44-IR700 for 1 h at 4°C. After washing with PBS, the cells were exposed to NIR light (690 nm, 100 mW/cm). At 1 h after light exposure, the cells were stained with 1 μg/mL PI. The dead cell percentage was analyzed using flow cytometry.

2.6 | Animals and tumor models

All in vivo procedures were conducted in compliance with the Guide for the Care and Use of Laboratory Animal Resources (1996), US National Research Council, and approved by the local Animal Care and Use Committee. Six- to eight-wk-old female C57BL/6 mice were purchased from the Jackson Laboratory (Bar Harbor, ME, USA). MOC2-luc cells (1×10^5) were inoculated into the submucosal layer of the right buccal mucosa (Figure 1A). All in vivo procedures were performed under anesthesia using inhaled 2%-5% isoflurane and/or intraperitoneal injection of 0.75 mg of sodium pentobarbital (Ovation Pharmaceuticals, Deerfield, IL, USA).

2.7 | Flow cytometric analysis

A single cell suspension was prepared. The cells were stained with antibodies; anti-CD31(clone 390; BioLegend, San Diego, CA, USA), anti-CD44 (clone IM7; Thermo Fisher Scientific), anti-CD45 (clone 30-F11; Thermo Fisher Scientific), and anti-CD140a (clone 135 905; BioLegend). To distinguish the dead cells, the cells were also stained with Fixable Viability Dye (Thermo Fisher Scientific). The fluorescence signal was analyzed using a flow cytometer (FACSLyric) and FlowJo software.

2.8 | Endoscopic observation

The tumor was observed with an endoscopic system and MACASO software (tentative name; Olympus, Tokyo, Japan) optimized for NIR-PIT.[17] An endoscope (BF TYPE P60; Olympus) was inserted into
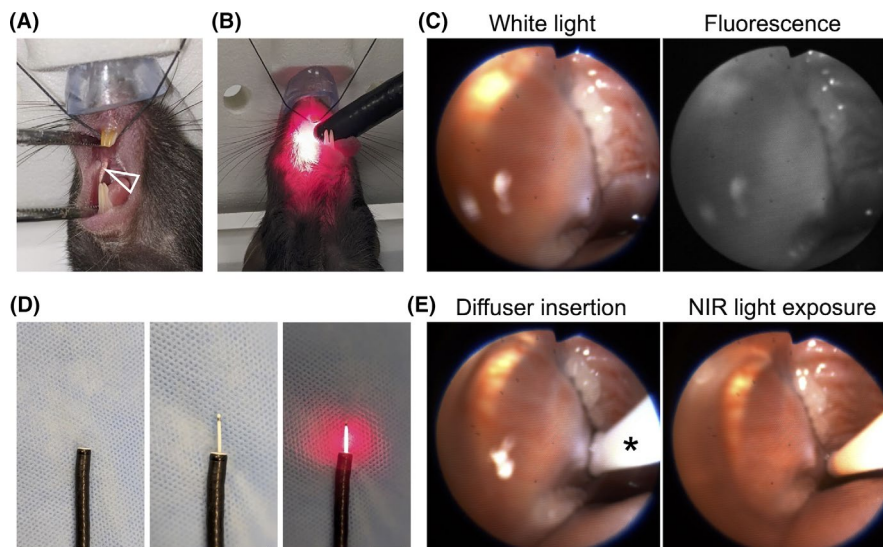

FIGURE 1 Endoscopic procedures. A, MOC2-luc cells were inoculated into the submucosal layer of the right buccal mucosa (arrowhead). B, An endoscope was inserted into the oral cavity. C, White light image and fluorescence image for IR700 are simultaneously displayed. D, A cylindrical light diffuser was inserted through the instrument channel of an endoscope. The diffuser was controlled by the endoscope. Left: tip of the endoscope, middle: inserted cylindrical diffuser, right: light exposure. Scale bars, 10 mm. E, In vivo NIR-PIT. The light diffuser (*) was inserted (left) and the right buccal region was exposed to NIR light (right)

the oral cavity (Figure 1B). The white light image was detected with a charged-coupled device (CCD) camera (FLIR Integrated Imaging Solutions, BC, Canada) and the fluorescence image was detected with an electron multiplying CCD (EM-CCD) camera (Hamamatsu Photonics, Shizuoka, Japan) using a light source (CLV-S190, Olympus Medical Systems) equipped with a multiband (400-486 nm and 550-666 nm) excitation filter and a 696-736 nm band pass emission filter. White light images and fluorescence images were simultaneously displayed on a monitor (Figure 1C, Video S1). Camera gain and exposure time were held constant throughout the experiment. For quantitative fluorescence analysis, region of interest (ROI) was set on the tumor. RFI was calculated from mean fluorescence intensity (MFI) as (MFI of measured time point)/(MFI of pre-injection status).

2.9 | In vivo NIR-PIT

Tumor bearing mice were randomized into 3 experimental groups: (1) no-treatment (control group), (2) intravenous (IV) injection of anti-CD44-IR700 (100 μg) without NIR light exposure (APC-IV group), and (3) IV injection of anti-CD44-IR700 (100 μg) followed by NIR light exposure (NIR-PIT group). At 5 d after tumor inoculation in the mice, the APC was administered. The tumor was exposed to NIR light the next day using an RD30 cylindrical diffuser (Medlight) inserted through the instrument channel of the endoscope (Figure 1D). The cylindrical diffuser was controlled by the endoscope. NIR light (690 nm, 100 mW/cm, 30 J/cm) was applied with an ML7710 laser system (Modulight) (Figure 1E; Video S2).

2.10 | Bioluminescence imaging

Luciferase activity was measured before and 6 h after the light exposure. D-Luciferin (15 mg/mL, 200 μL; Gold Biotechnology, St. Louis, MO, USA) was injected intraperitoneally and luciferase activity was analyzed with a Photon Imager and M3 Vision Software (Biospace Laboratory, Paris, France). The ROI was drawn to include the entire head and counts per minute of relative light units (RLU) were calculated. Relative luciferase activity was calculated as (RLU at 6 h after the light exposure)/(RLU prior to the light exposure).

2.11 | Histological analysis

Tumors were harvested 6 h after NIR light exposure. Extracted tumors were fixed with 10% formalin, embedded in paraffin, thinly sliced and stained with hematoxylin and eosin (H&E).

2.12 | Statistical analysis

Data are expressed as means ± SEM. Statistical analysis was performed using GraphPad Prism software (GraphPad Software, La

Jolla, CA, USA). For one-time measurements, a one-way ANOVA followed by Tukey test was used. For comparison of fluorescence intensity, a repeated measures two-way ANOVA followed by Tukey test was used. A P-value of less than .05 was considered significant.

3 | RESULTS

3.1 | Anti-CD44-IR700 specifically bound to MOC2-luc cells

To assess if anti-CD44-IR700 was bound to MOC2-luc cells, the cells were incubated with the anti-CD44-IR700 and the fluorescence signal was analyzed with flow cytometry. MOC2-luc cells showed a fluorescence shift after incubation with anti-CD44-IR700 (Figure 2A). This fluorescence shift was completely blocked with excess unconjugated anti-CD44 antibody. These results verified the specific binding of anti-CD44-IR700 to MOC2-luc cells.

3.2 | CD44-targeted NIR-PIT kills MOC2-luc cells

To determine if CD44-targeted NIR-PIT killed MOC2-luc cells, the cells were incubated with anti-CD44-IR700 and exposed to NIR light with a cylindrical diffuser. Cell morphology was observed under a microscope. MOC2-luc cells showed bleb formation and swelling then ruptured within a few minutes of light exposure, accompanied by loss of fluorescence (Figure 2B). Cytotoxicity was quantitatively assessed with flow cytometry using PI staining (Figure 2C). The percentage of PI-stained dead cells increased after the NIR-PIT in a light dose-dependent manner. Administration of anti-CD44-IR700 alone or irradiation of NIR light alone did not result in cytotoxicity. These results verified the in vitro therapeutic efficacy of CD44-targeted NIR-PIT against MOC2-luc cells.

3.3 | CD44 is expressed in vivo on orthotopic MOC2-luc tumors

To assess if CD44 is expressed on MOC2-luc cells within established tumors, tumors were extracted and flow cytometrically analyzed. CD45⁻CD31⁻CD140a⁻ cancer cells showed surface expression of CD44 (Figure S1).

3.4 | Loss of IR700 fluorescence during NIR-PIT was successfully detected with fluorescence endoscopy

To assess if the fluorescence signal of IR700 was quantitatively altered during NIR-PIT, fluorescence endoscopy was performed. Mice with orthotopic tumor allografts were randomized into 3 groups: no-treatment (control), IV injection of anti-CD44-IR700 without NIR light exposure (APC-IV), and IV injection of

FIGURE 2 In vitro NIR-PIT. A, Binding of anti-CD44-IR700 to cultured MOC2-luc cell line was assessed with flow cytometry. Unconjugated anti-CD44 antibody was added to some samples to verify the specific binding. B, Microscopic observation of the MOC2-luc cells during in vitro NIR-PIT. Scale bars, 20μm. Differential interference contrast (DIC) images and fluorescence image for IR700 were obtained. C, Quantitative cytotoxicity assessment of in vitro NIR-PIT. Dead cell percentage was analyzed using propidium iodide (PI) staining and flow cytometry. Histograms show a representative fluorescence of the PI signal for each experimental setting. Bar graphs show the PI-stained dead cell percentages (n = 4; one-way ANOVA followed by Tukey test; ****$P < .0001$)
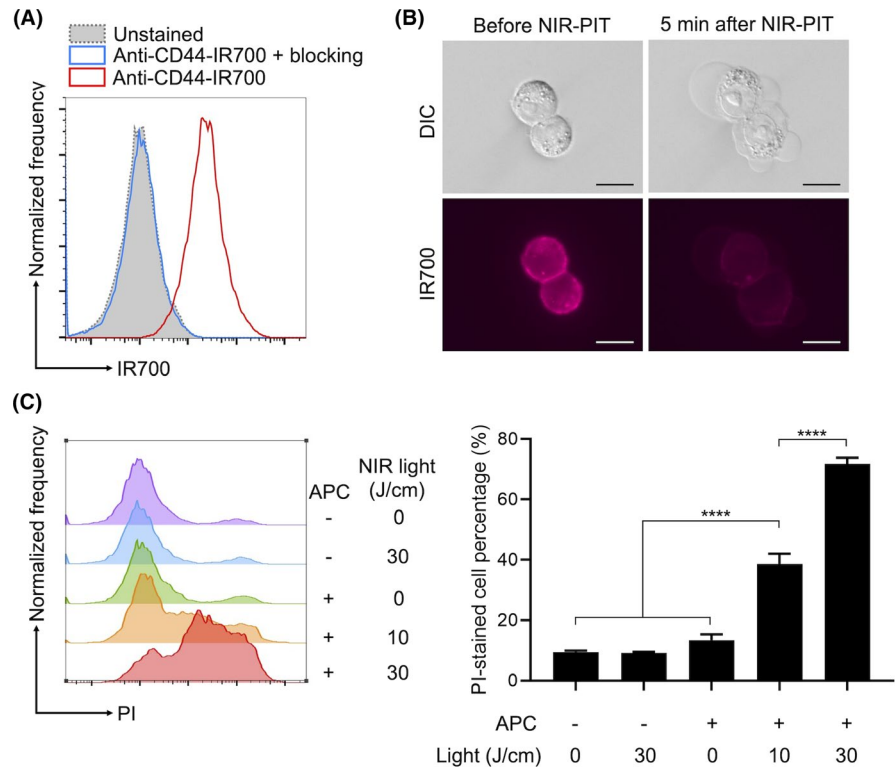
anti-CD44-IR700 followed by NIR light exposure (NIR-PIT). Fluorescence endoscopy was performed before the APC injection and before and after the NIR light exposure (Figure 3A). Orthotopic MOC2-luc tumors were established in the right buccal mucosa and endoscopically observed (Figure 3B). Real-time fluorescence images were displayed and captured at 3 time points (Figure 3C). In the APC-IV group and NIR-PIT group, the RFI of tumor was significantly higher compared with the control group before light exposure; the fluorescence signal was attenuated only in NIR-PIT group whereas no significant change was shown in the APC-IV group (Figure 3D). These results demonstrated that this fluorescence endoscopy system could quantitatively measure changes in IR700 fluorescence in real time.

3.5 | In vivo NIR-PIT showed therapeutic efficacy

To verify the in vivo therapeutic efficacy of endoscopic NIR-PIT, luciferase activity was assessed with bioluminescence imaging (BLI). Six h after the light exposure, luciferase activity of oral tumor was significantly lower in the NIR-PIT group compared with the other 2 groups (Figure 4). To assess the morphological changes, tumors from each experimental group were extracted 6 h after light exposure and stained with H&E (Figure 5). In the NIR-PIT group, cancer cells and nuclei were observed to shrink compared with the control group, although no obvious histological change was observed in the APC-IV group. These results verified the in vivo therapeutic effects of endoscopic NIR-PIT in an orthotopic HNC model.

4 | DISCUSSION

We have demonstrated the feasibility of using endoscopic NIR-PIT against HNC in an orthotopic animal model. Moreover, we demonstrate the potential usefulness of an integrated quantitative fluorescence imaging system in the endoscopic camera. Endoscopic NIR-PIT induced necrotic cell death in cancer cells as confirmed by BLI and histological analysis. As NIR-PIT against inoperable recurrent HNCs has already been conditionally approved in Japan, we demonstrate the potential use of endoscopic NIR-PIT as a means of delivering NIR light and assessing treatment in real time with quantitative fluorescence. While it is possible to perform NIR-PIT and quantitative fluorescence without endoscopy, the convenience of having both a light delivery and fluorescence imaging device in 1 instrument is compelling for clinical translation. The endoscope used in this study was a bronchoscope for human use, therefore it can reach deep inside human body. Also, this technology could be applied to gastrointestinal endoscopy.

Recently, early stage HNCs, including superficial cancers or carcinoma in situ, have become detectable with advanced endoscopic technology, such as narrow band imaging (NBI)[19-21] or linked color imaging (LCI).[22] For these early stage cancers, endoscopic surgeries can be performed as less invasive alternatives to conventional surgery.[6] Endoscopic NIR-PIT has the potential to be applied to such early stage HNCs as well. Short treatment time (5-6 min) is one of the advantages of this therapy, and may result in a shorter recovery time.

Fluorescence imaging during NIR-PIT is a useful tool for assessing the completeness of light exposure and therefore efficacy.
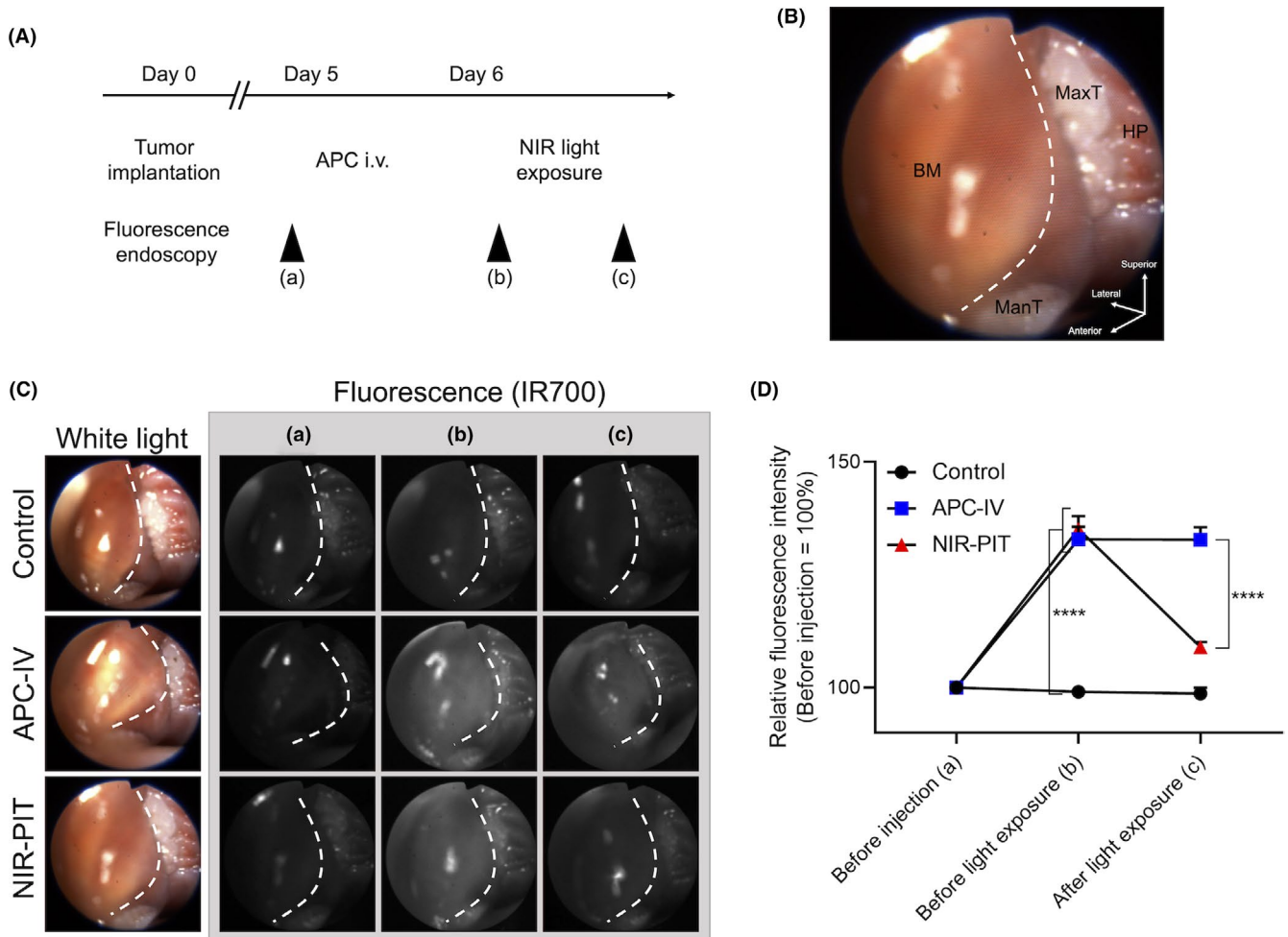
FIGURE 3 Quantitative fluorescence analysis during the endoscopic NIR-PIT. A, Treatment and imaging schedule. B, Orientation of white light image. Right buccal region was observed. BM, buccal mucosa; HP, hard palatine; ManT, mandibular teeth; MaxT, maxillary teeth. White dotted line represents the outline of the tumor. C, The representative image of each experimental group at each observed time point. White dotted line represents the outline of the tumor. D, Relative fluorescence intensity was calculated from the mean fluorescence intensity of the tumor (n = 10; repeated measures two-way ANOVA followed by Tukey test; ****P < .0001)

Theranostic APCs used in NIR-PIT have no therapeutic effect without NIR light exposure. Therefore, complete geographic and temporal coverage of tumor by NIR light is required.[16,23] It has been reported that NBI enables more accurate diagnosis of HNC compared with white light imaging alone.[20] Adding fluorescence imaging of IR700 might provide more accurate information on tumor location with which to direct NIR-PIT. Also, sufficient light exposure is necessary for satisfactory results from NIR-PIT.[18] Therapeutic efficacy of NIR-PIT correlates with the degree of fluorescence loss by IR700 on the APC, therefore, intraprocedural real-time monitoring is possible when measuring IR700 fluorescence during treatment. IR700 fluorescence loss during NIR-PIT has been previously demonstrated in subcutaneous tumors in which off-peak IR700 fluorescence was measured using a clinically approved camera designed for indocyanine green (ICG).[24] The endoscopic system used in the current study provides real-time quantitative fluorescence information. If the treated tumor reveals residual fluorescence after light exposure, additional NIR light could be applied as needed. Endoscopic local NIR-PIT could also be applied as neoadjuvant or

adjuvant therapy for endoscopic resection and could also be used intraoperatively.

In the past few decades, endoscopic surgery in the head and neck region has been rapidly expanding in the form of minimally invasive surgeries; transoral robotic surgery (TORS),[25] transoral video laryngoscopic surgery (TOVS),[26] and endoscopic laryngo-pharyngeal surgery (ELPS).[6] Associated devices include multiarm retractors or curved laryngoscopes, which provide the operator excellent visualization of the field. Using these devices, endoscopic NIR-PIT could be applied to a broad range of tumors in the head and neck region with maximal organ preservation, improving recovery time and quality of life.

Patients with HNC often experience synchronous or metachronous secondary cancers in the upper aerodigestive tract, including the esophagus and lung, at rates of 9.4%-14.2%.[27,28] Unlike radiotherapy, NIR-PIT does not have a limitation with regard to repeated therapy.[29] Therefore, endoscopic NIR-PIT could be useful in such secondary cancers. Even in primary tumors, if the initial treatment is only partially successful, repeated endoscopic NIR-PITs can be

FIGURE 4 Bioluminescence imaging (BLI). In vivo cytotoxicity of the NIR-PIT was quantitatively assessed with luciferase activity 6 h after the light exposure. Upper: representative result of BLI for each experimental group. The mice were in lateral position. White dotted line represents the outline of the murine body. Lower: Relative luciferase activity (n = 10; one-way ANOVA followed by Tukey test; *P < .05)
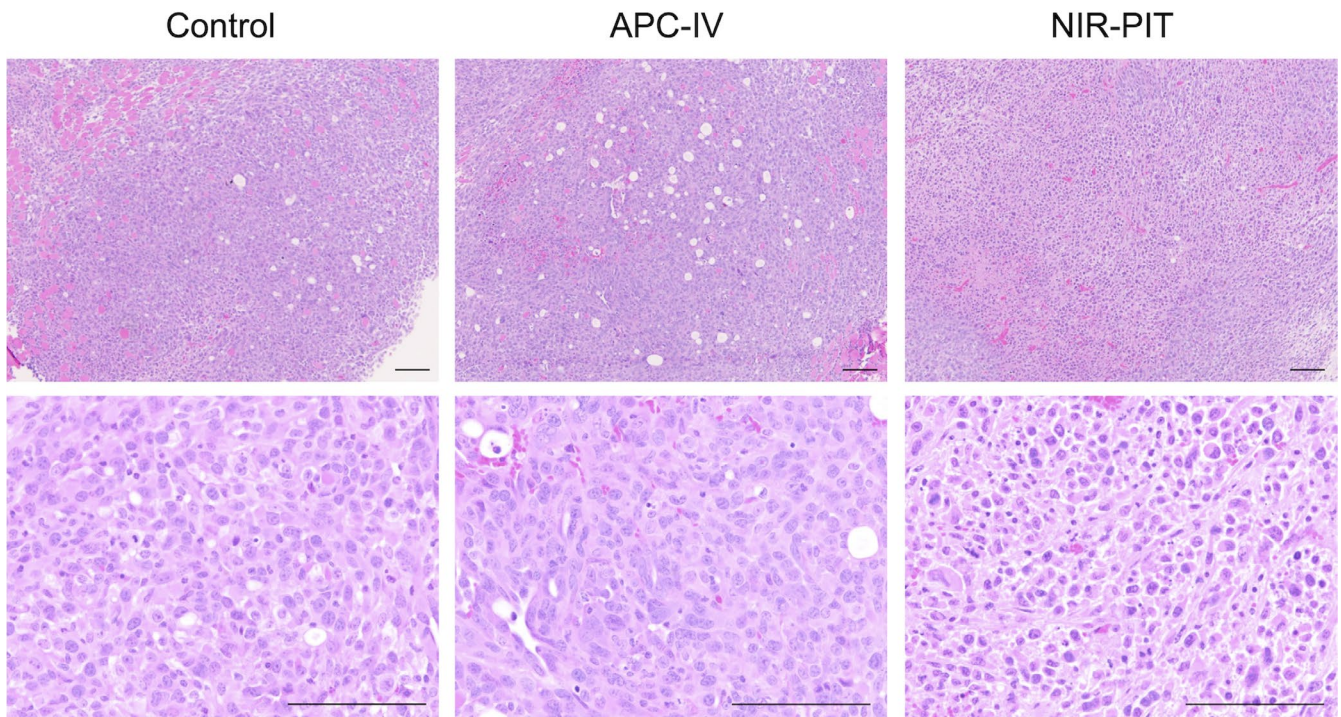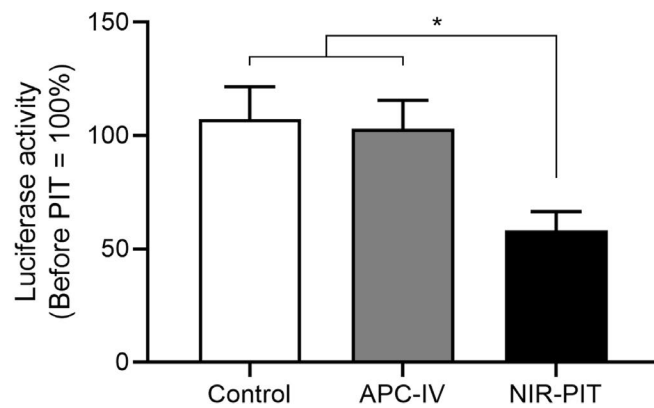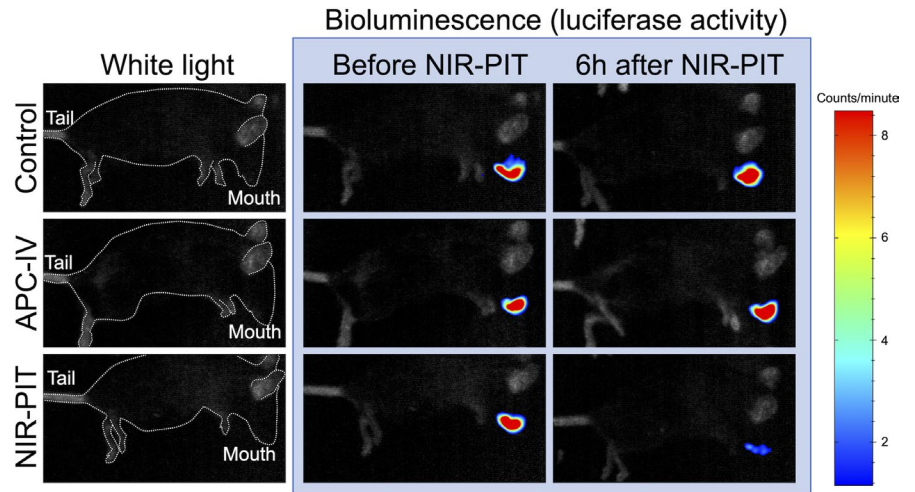

FIGURE 5 Histological analysis. Tumors were extracted 6 h after light exposure and stained with H&E stain. In the NIR-PIT group, cellular and nuclear shrinkage of the cancer cell was observed. Scale bars, 100 μm

performed on the same site at a later time. In mouse models, cancer cell-targeted NIR-PIT has been proved to enhance antitumor immune response by releasing various kinds of tumor-associated antigens (TAAs),[30,31] that could help to treat satellite or distant lesions. Repeated NIR-PITs could work as immune boosters, although such effects are currently investigated.

There are several limitations to this study. First, CD44 is not a typical cancer cell-specific marker; it is also expressed on immune and epithelial cells. The latter cells create background fluorescence that can interfere with lesion detection. A more cancer-specific antibody might result in higher tumor to background signal ratios. Second, we used firefly luciferase bioluminescence in this study to assess in vivo therapeutic efficacy because it reflects early NIR-PIT effect superior to fluorescence imaging.[32] However, imaging resolution would be higher with fluorescent proteins compared with luciferase.[33,34] Third, only a single cell line was used. However, the major purpose of this work was to demonstrate the feasibility of combining endoscopic NIR-PIT with quantitative real-time fluorescence imaging in a HNC rather than demonstrating a broad range of efficacy across many cell lines. Using this system, endoscopic NIR-PIT could be readily adapted to clinical use.

In conclusion, endoscopic NIR-PIT with quantitative fluorescence imaging showed in vivo therapeutic efficacy. This treatment could be readily combined with endoscopic tumor resection. Quantitative fluorescence imaging could help to tailor light dosimetry to each subject during NIR-PIT. This treatment could also be applied to other cancers that are approachable by endoscopy.

CONFLICT OF INTEREST
The authors have no conflict of interest to disclose.

ORCID
Ryuhei Okada https://orcid.org/0000-0003-3589-5054
Fuyuki Inagaki https://orcid.org/0000-0002-9953-3805
Hiroaki Wakiyama https://orcid.org/0000-0001-6388-9888
Hisataka Kobayashi https://orcid.org/0000-0003-1019-4112

REFERENCES
1. Chow LQM. Head and Neck Cancer. *N Engl J Med*. 2020;382:60-72.
2. Sung H, Ferlay J, Siegel RL, et al. Global Cancer Statistics 2020: GLOBOCAN Estimates of Incidence and Mortality Worldwide for 36 Cancers in 185 Countries. *Cancer J Clin*. 2021;71(3):209-249.
3. Bonner JA, Harari PM, Giralt J, et al. Radiotherapy plus cetuximab for squamous-cell carcinoma of the head and neck. *N Engl J Med*. 2006;354:567-578.
4. Ferris RL, Blumenschein G Jr, Fayette J, et al. Nivolumab for Recurrent Squamous-Cell Carcinoma of the Head and Neck. *N Engl J Med*. 2016;375:1856-1867.
5. Goh HK, Ng YH, Teo DT. Minimally invasive surgery for head and neck cancer. *Lancet Oncol*. 2010;11:281-286.
6. Tateya I, Shiotani A, Satou Y, et al. Transoral surgery for laryngopharyngeal cancer - The paradigm shift of the head and cancer treatment. *Auris Nasus Larynx*. 2016;43:21-32.
7. Mitsunaga M, Ogawa M, Kosaka N, Rosenblum LT, Choyke PL, Kobayashi H. Cancer cell-selective in vivo near infrared photoimmunotherapy targeting specific membrane molecules. *Nat Med*. 2011;17:1685-1691.
8. Ogawa M, Tomita Y, Nakamura Y, et al. Immunogenic cancer cell death selectively induced by near infrared photoimmunotherapy initiates host tumor immunity. *Oncotarget*. 2017;8:10425-10436.
9. Sato K, Sato N, Xu B, et al. Spatially selective depletion of tumor-associated regulatory T cells with near-infrared photoimmunotherapy. *Sci Transl Med*. 2016;8:352ra110.
10. Chen J, Zhou J, Lu J, Xiong H, Shi X, Gong L. Significance of CD44 expression in head and neck cancer: a systemic review and meta-analysis. *BMC Cancer*. 2014;14:15.
11. de Jong MC, Pramana J, van der Wal JE, et al. CD44 expression predicts local recurrence after radiotherapy in larynx cancer. *Clin Cancer Res*. 2010;16:5329-5338.
12. Motegi A, Fujii S, Zenda S, et al. Impact of expression of CD44, a cancer stem cell marker, on the treatment outcomes of intensity modulated radiation therapy in patients with oropharyngeal squamous cell carcinoma. *Int J Radiat Oncol Biol Phys*. 2016;94:461-468.
13. Nagaya T, Nakamura Y, Okuyama S, et al. Syngeneic Mouse Models of Oral Cancer Are Effectively Targeted by Anti-CD44-Based NIR-PIT. *Mol Can Res*. 2017;15:1667-1677.
14. Wakiyama H, Furusawa A, Okada R, et al. Increased immunogenicity of a minimally immunogenic tumor after cancer-targeting near infrared photoimmunotherapy. *Cancers*. 2020;12:3747.
15. Hoffman RM. Patient-derived orthotopic xenografts: better mimic of metastasis than subcutaneous xenografts. *Nat Rev Cancer*. 2015;15:451-452.
16. Inagaki FF, Fujimura D, Furusawa A, et al. Diagnostic imaging in near-infrared photoimmunotherapy using a commercially available camera for indocyanine green. *Cancer Sci*. 2021;112(3):1326-1330.
17. Nagaya T, Okuyama S, Ogata F, Maruoka Y, Choyke PL, Kobayashi H. Endoscopic near infrared photoimmunotherapy using a fiber optic diffuser for peritoneal dissemination of gastric cancer. *Cancer Sci*. 2018;109:1902-1908.
18. Mitsunaga M, Nakajima T, Sano K, Kramer-Marek G, Choyke PL, Kobayashi H. Immediate in vivo target-specific cancer cell death after near infrared photoimmunotherapy. *BMC Cancer*. 2012;12:345.
19. Muto M, Horimatsu T, Ezoe Y, Morita S, Miyamoto S. Improving visualization techniques by narrow band imaging and magnification endoscopy. *J Gastroenterol Hepatol*. 2009;24:1333-1346.
20. Muto M, Minashi K, Yano T, et al. Early detection of superficial squamous cell carcinoma in the head and neck region and esophagus by narrow band imaging: a multicenter randomized controlled trial. *J Clin Oncol*. 2010;28:1566-1572.
21. Muto M, Nakane M, Katada C, et al. Squamous cell carcinoma in situ at oropharyngeal and hypopharyngeal mucosal sites. *Cancer*. 2004;101:1375-1381.
22. Ono S, Kawada K, Dohi O, et al. Linked Color Imaging Focused on Neoplasm Detection in the Upper Gastrointestinal Tract : A Randomized Trial. *Ann Intern Med*. 2021;174:18-24.
23. Inagaki FF, Fujimura D, Furusawa A, et al. Fluorescence Imaging of Tumor-Accumulating Antibody-IR700 Conjugates Prior to Near-Infrared Photoimmunotherapy (NIR-PIT) Using a Commercially Available Camera Designed for Indocyanine Green. *Mol Pharm*. 2021;18:1238-1246.
24. Okuyama S, Fujimura D, Inagaki F, et al. Real-time IR700 fluorescence imaging during near-infrared photoimmunotherapy using a clinically-approved camera for indocyanine green. *Cancer Diagnos Prog*. 2021;1:29-34.

25. Nakayama M, Holsinger FC, Chevalier D, Orosco RK. The dawn of robotic surgery in otolaryngology-head and neck surgery. *Jpn J Clin Oncol.* 2019;49:404-411.

26. Tomifuji M, Araki K, Yamashita T, Shiotani A. Transoral videolaryngoscopic surgery for oropharyngeal, hypopharyngeal, and supraglottic cancer. *Eur Archiv Oto-Rhino-Laryngol.* 2014;271:589-597.

27. Bugter O, van Iwaarden DLP, Dronkers EAC, et al. Survival of patients with head and neck cancer with metachronous multiple primary tumors is surprisingly favorable. *Head Neck.* 2019;41:1648-1655.

28. Priante AV, Castilho EC, Kowalski LP. Second primary tumors in patients with head and neck cancer. *Curr Oncol Rep.* 2011;13:132-137.

29. Kobayashi H, Choyke PL. Near-Infrared Photoimmunotherapy of Cancer. *Acc Chem Res.* 2019.52:2332–2339.

30. Nagaya T, Friedman J, Maruoka Y, et al. Host Immunity Following Near-Infrared Photoimmunotherapy Is Enhanced with PD-1 Checkpoint Blockade to Eradicate Established Antigenic Tumors. *Cancer Immunol Res.* 2019;7:401-413.

31. Okada R, Furusawa A, Vermeer DW, et al. Near-infrared photoimmunotherapy targeting human-EGFR in a mouse tumor model simulating current and future clinical trials. *EBioMedicine.* 2021;67:103345.

32. Maruoka Y, Nagaya T, Nakamura Y, et al. Evaluation of Early Therapeutic Effects after Near-Infrared Photoimmunotherapy (NIR-PIT) Using Luciferase-Luciferin Photon-Counting and Fluorescence Imaging. *Mol Pharm.* 2017;14:4628-4635.

33. Hoffman RM. The multiple uses of fluorescent proteins to visualize cancer in vivo. *Nat Rev Cancer.* 2005;5:796-806.

34. Hoffman RM, Yang M. Whole-body imaging with fluorescent proteins. *Nat Protoc.* 2006;1:1429-1438.

SUPPORTING INFORMATION

Additional supporting information may be found online in the Supporting Information section.